Suppression of single-molecule conductance fluctuations using extended anchor groups on graphene and carbon-nanotube electrodes

Csaba G. Péterfalvi and Colin J. Lambert*

Department of Physics, Lancaster University, Lancaster, LA1 4YB, United Kingdom

(Received 30 April 2012; revised manuscript received 25 June 2012; published 23 August 2012)

Devices formed from single molecules attached to noble-metal electrodes exhibit large conductance fluctuations, which inhibit their development as reproducible functional units. We demonstrate that single molecules with planar anchor groups attached to carbon-based electrodes are more resilient to atomic-scale variation in the contacts and exhibit significantly lower conductance fluctuations. We examine the conductance of a 2,6-dibenzylamino core-substituted naphthalenediimide chromophore attached to carbon electrodes by either phenanthrene anchors or more extended anchor groups, which include oligophenylene ethynylene spacers. We demonstrate that for the more spatially extended anchor groups conductance fluctuations are significantly reduced. The current-voltage characteristic arising from long-range tunneling is found to be strongly nonlinear with pronounced conductance suppression below a threshold voltage of approximately 2.5 V.

DOI: 10.1103/PhysRevB.86.085443 PACS number(s): 72.80.Vp, 31.15.ae, 31.15.at, 71.15.Mb

I. INTRODUCTION

Combined experimental and theoretical studies have provided new insights into the interplay of molecular conformation, electronic structure, and electrical conductance[1] in single-molecule electronic devices. It is clear that measured conductance values depend on the atomic-scale contact geometry of the electrodes,[2] temperature,[3] the local environment of the system[4] (vacuum or air, solvent, etc.), and molecular features such as the extent of conjugation,[5,6] the nature of the terminal anchor groups[7] (e.g., thiol, amine, carboxylic acid), the detailed conformation[8] and tilt angle[9] of the molecule in the junction, and the quantum coherence and interference of electrons transiting the molecule.[10,11]

With a view to developing stable sub-10-nm electronic devices, a great deal of effort has been devoted to understanding the interplay between terminal anchor groups and metallic electrodes. The ideal molecular anchor group should form reproducible and mechanically stable contacts with well-defined binding sites and strong electronic coupling to the nanoelectrodes.[12] Recently, chemical synthesis was used to vary the anchor groups within a family of molecules and the relative anchoring performance of four different terminal groups [SH, pyridyl (PY), NH_2, and CN] was measured and calculated. This study revealed the following sequence for junction formation probability and stability: PY > SH > NH_2 > CN.[13] In common with other studies of single molecules attached to gold electrodes, broad variations in the measured conductances are observed, which suggests that alternative electrodes to gold are needed, if reliable and reproducible devices are to be developed.[5] Alternatives based on surface grafting via covalent bonds, such as carbon-carbon,[14] metal-carbon,[15] and silicon-carbon,[16] also exhibit significant sample-to-sample fluctuations.

In this paper, as a possible route to reducing fluctuations, we examine the use of extended planar anchor groups attached via π-π interactions to either graphene or carbon-nanotube (CNT) electrodes. Recent experiments suggest that carbon-based electrodes are a viable alternative to the more commonly used noble metals.[17,18] For example, Prins *et al.*[18] created a few-nanometer-wide gap in graphene, via feedback-controlled electroburning and carried out room-temperature, gate-controlled measurements on a single molecule bridging the gap. Similarly Marquardt *et al.*[19] used electrical breakdown to form nanogaps in free-standing CNTs and bridged the gap with a single molecule.

Nanogap electrodes of this kind have several advantages over more commonly used noble-metal electrodes, because the absence of screening makes it easier to gate the molecule and their planar structure makes it possible to image the molecule *in situ*. In this paper, we perform simulations based on density-functional theory (DFT) to demonstrate that such carbon-based electrodes have the further advantage of allowing the suppression of conductance fluctuations arising from atomic-scale disorder by increasing the size of planar anchor groups.

As a specific example, we investigate the electronic properties of a rodlike molecule, closely related to that measured by Marquardt *et al.*,[19,20] which has a 2,6-dibenzylamino core-substituted naphthalenediimide (NDI) functional group, connected via oligophenylene ethynylene (OPE) linkers to phenanthrene terminal groups, as shown in Fig. 1. This contains the same NDI core as the molecule measured by Marquardt *et al.*, but theirs contains three OPEs in the left and right linkers, whereas the molecule in Fig. 1 contains only a single OPE in each linker. The longer 3-3 OPE molecule of Ref. 19, when attached to electrodes, is prohibitively expensive to simulate, whereas the 1-1 OPE of Fig. 1 is more tractable.

To model carbon-based electrodes, we couple the planar end groups of the molecule of Fig. 1 to large-diameter (12,12) single-walled, metallic armchair CNT electrodes, via π overlap, as shown in Fig. 1. Since the CNTs are locally flat on the scale of the phenanthrene terminal groups and OPE bridge, our results also capture generic transport properties obtained using alternative carbon-based electrodes, such as multiwall CNTs and mono- or few-layer graphene.

Our first goal is to compute the I-V characteristics of this molecule, and show that the threshold voltage measured by Marquardt *et al.* is an intrinsic property of this class of

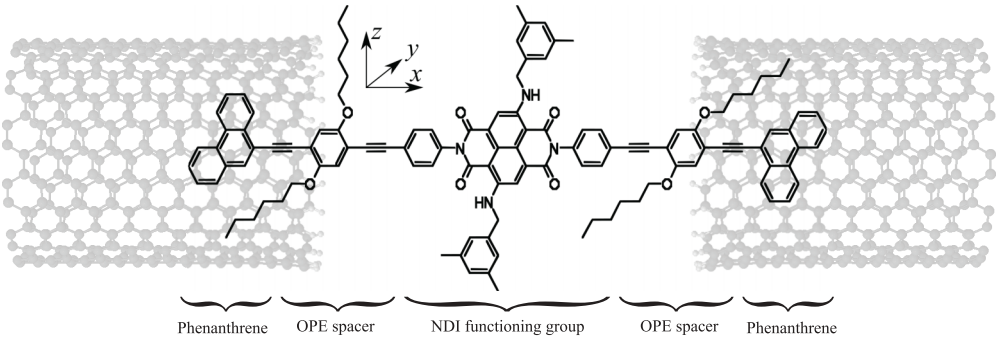

FIG. 1. The studied molecule with an NDI functioning group, OPE spacers, and phenanthrene anchor groups on the top of the CNT junction (shown in light gray).

molecule. Our second goal is to show that by increasing the size of the planar anchor groups, the sensitivity to lattice defects can be reduced.

II. THEORETICAL METHOD

The structure shown in Fig. 1 involves over 1100 atoms and therefore an efficient computational scheme is needed to determine its electrical properties. The first step is to calculate the relaxed geometry, for which we use the DFT code SIESTA.[21] A double-ζ polarized basis set is chosen, the exchange correlation is described with the generalized gradient approximation[22] (GGA), and the atoms are relaxed until all forces are less than 0.0 eV/Å. The size of our molecules prevents the inclusion of van der Waals interaction within a currently tractable calculation. Nevertheless, it is known that van der Waals interactions tend to increase the binding energy of smaller molecules to electrodes, and the effect on transmission is to make the anchor groups more transparent. In our case however, the transmission is dominated by tunneling through the gap between the highest occupied and the lowest unoccupied molecular orbitals (HOMO and LUMO) and therefore increasing the transparency of the contacts is not likely to produce a significant change. The relaxation consists of several steps: the CNT leads and the molecule are relaxed separately, and then the whole system is again relaxed. After introducing lattice defects into the once-relaxed system, the structure is again relaxed. For consistency, the same force tolerance is used in all cases.[23]

For the purpose of structure relaxation, the system is infinitely periodic along the x axis and for the small (large) end groups comprises nanotube sequences between the molecules made up of 17 (21) CNT unit cells. These are long enough to ensure convergence of the mean-field DFT Hamiltonian parameters, which are later employed to compute transmission coefficients. On the surfaces of the nanogaps, the (12,12)

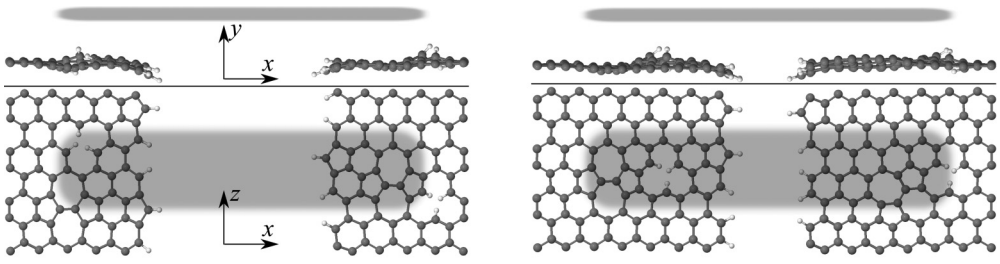

(a) Small contacts with few defects

(b) Large contacts with few defects

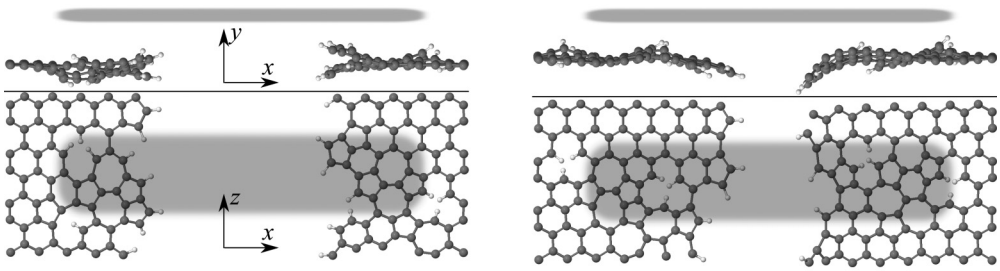

(c) Small contacts with more defects

(d) Large contacts with more defects

FIG. 2. Projections of the contact area to the x-z plane, viewed from above and from the side. The gray shading represents the molecule above it. The gap and the middle section of the molecule are shrunk to fit the figure.

armchair CNTs are terminated with hydrogen atoms to saturate the dangling bonds.

After relaxing the whole periodic system, the underlying DFT tight-binding Hamiltonian is extracted, within a double-ζ basis-set representation and the transmission coefficient $T(E)$ is calculated using an equilibrium implementation of the *ab initio* transport code SMEAGOL,[24] which is based on a Greens-function scattering technique. At temperature T and bias V, the current I can be calculated using the integral

$$I(V) = \frac{2e}{h}\int_{-\infty}^{\infty}[f(E - eV/2) - f(E + eV/2)]T(E)dE,$$

where $f(E)$ is the Fermi function.

III. LATTICE DEFECT RESILIENCE

To show that extended anchor groups make the system resilient to lattice defects, we introduce defects in the lattice of the CNT electrodes mainly around the anchor groups, and allow the bulk of the CNT to remain pristine. We introduce defects in two stages: first, we remove 6-6 carbon atoms from the edges, and introduce 1-1 *Stone-Wales defects*[25] and 1-1 vacancies in the contact region of each electrode, which consists of the last couple of unit cells in the vicinity of the end of the CNT. In the second stage, we double the concentration of each kind of defect. In the presence of such defects, the relaxed geometries of the CNT surfaces in the vicinity of the anchor groups are shown in Fig. 2, where for clarity, both side and top views are shown and the attached molecule is represented simply by gray shaded regions.

To demonstrate that fluctuations are reduced in the presence of more extended anchor groups, we consider the cases of "small" and "large" anchor groups. The small-anchor configuration is shown in Fig. 1, where only the phenanthrene group is in direct contact with the CNT. For the large anchor group, we consider the case where the OPE spacers also overlay the CNT. We consider the cases of small and large anchors attached to CNTs containing no defects (which we label $j = 1$) and two nonzero concentrations of defects, (which we label $j = 2,3$) and compute the transmission and current-voltage curves $I_j^{\text{small}}(V)$ and $I_j^{\text{large}}(V)$, shown in Fig. 3. Interestingly, above 3 V, we find that lattice defects increase the electrical conductance, by broadening the Breit-Wigner resonances around ± 1.5 V. This is particularly striking for the small anchor groups.

To quantify the conductance fluctuations of the results presented in Figs. 3(b) and 3(d), at each voltage V, we compute the finite-voltage conductances $g_j^{\text{small}}(V) = I_j^{\text{small}}(V)/V$ and $g_j^{\text{large}}(V) = I_j^{\text{small}}(V)/V$ for each of the three curves in Figs. 3(b) and 3(d). At each voltage, we then compute the means $g^{\text{small}}(V) = (1/3)\sum_{j=1}^{3} g_j^{\text{small}}(V)$ and $g^{\text{large}}(V) = (1/3)\sum_{j=1}^{3} g_j^{\text{large}}(V)$ and standard deviations $\sigma^{\text{small}}(V) = \sqrt{\{(1/3)\sum_{j=1}^{3}[g_j^{\text{small}}(V) - g^{\text{small}}(V)]^2\}}$ and $\sigma^{\text{large}}(V) = \sqrt{\{(1/3)\sum_{j=1}^{3}[g_j^{\text{large}}(V) - g^{\text{large}}(V)]^2\}}$ of each set

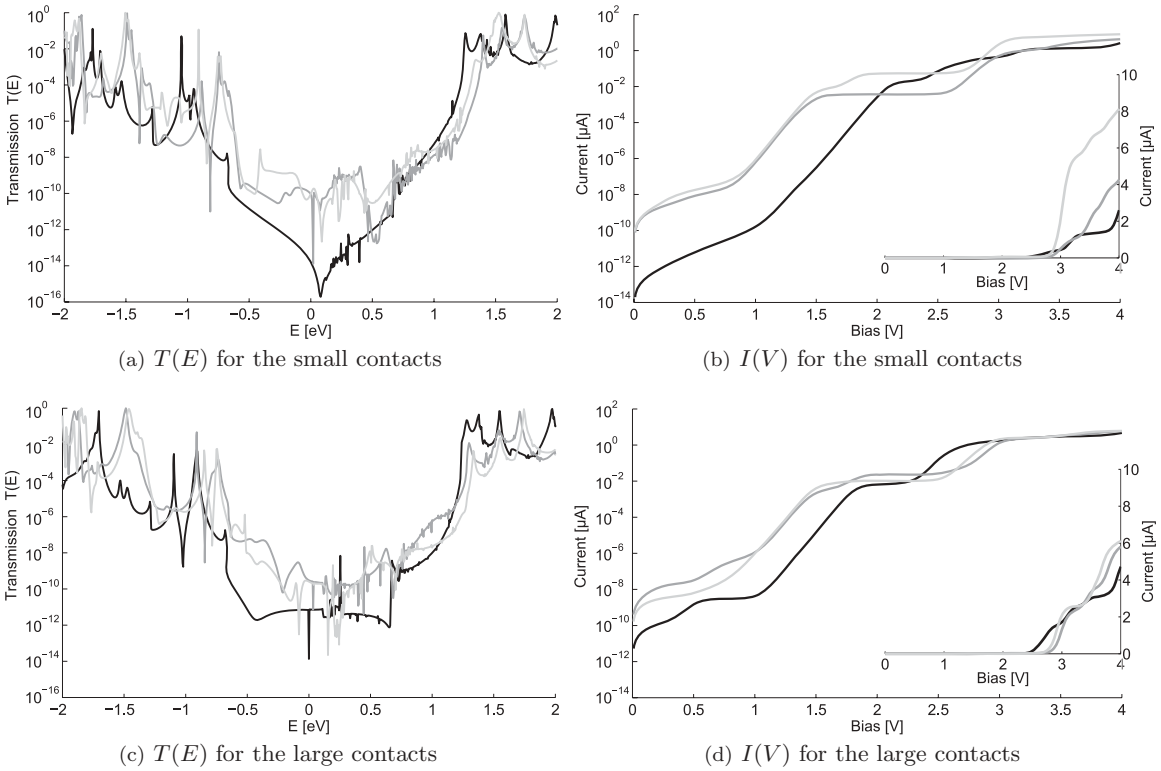

(a) $T(E)$ for the small contacts

(b) $I(V)$ for the small contacts

(c) $T(E)$ for the large contacts

(d) $I(V)$ for the large contacts

FIG. 3. Transport probability as a function of the energy and room-temperature current as a function of the applied bias voltage. The current is presented on a logarithmic scale and also on a linear scale in the inset. The black curve corresponds to perfect electrodes, dark gray to CNTs with a few defects, and light gray to CNTs with many defects. Note the *threshold* voltage below 3 V.

of three curves. As a measure of their relative conductance fluctuations over a given voltage window, we define the ratio

$$\alpha = \left(\int_{V_1}^{V_2} \sigma_{\text{small}}(V)dV\right) \Big/ \left(\int_{V_1}^{V_2} \sigma_{\text{large}}(V)dV\right). \quad (1)$$

When integrating from 0 up to 4 V, we find $\alpha = 3.7$, but when integrating only above the switch-on voltage from 3 to 4 V, we find $\alpha = 5.6$. Both cases clearly demonstrate that the $I(V)$ curves with large anchor groups are far more resilient to lattice defects than those with smaller anchor groups.

In common with the measured 3-3 OPE molecule,[19] we find that $I(V)$ curves of our 1-1 OPE are strongly nonlinear, with a threshold voltage for charge transport of V_{CT}, which supports the idea that this threshold voltage is an intrinsic feature of this class of molecules. The 3-3 OPE threshold voltage was measured to be ca. $V_{CT} = 2$ V, whereas in our case the 1-1 OPE threshold is predicted to be $V_{CT} = 2.5$–3 V. In our calculations, transport takes place by phase-coherent tunneling and since the Fermi energy is close to the center of the HOMO-LUMO gap, V_{CT} is approximately twice the value of the HOMO-LUMO gap, which is larger for the smaller molecule.

IV. CONCLUSIONS

Single-molecule electronics is an embryonic technology, whose development is hampered by conductance fluctuations due to atomic-scale variation at the contacts to electrodes. Using *ab initio* methods, we have demonstrated that conductance fluctuations of a single molecule bridging carbon-based electrodes can be significantly decreased by increasing the size of planar aromatic anchor groups, which π-π bond to the electrodes. As a specific example, we have examined the 2,6-dibenzylamino core-substituted naphthalenediimide (NDI) chromophore attached to carbon-nanotube electrodes, which is closely related to a molecule measured recently by Marquardt *et al.*[19] In agreement with their measurements, we find a nonlinear $I(V)$ with strong current suppression at low voltages. The agreement between their threshold and our numerical value is of course a coincidence, because the molecule measured by Marquardt *et al.*[19] is similar, but not identical, to ours. Furthermore, it is well known that DFT may not predict accurately the position of the Fermi energy relative to the HOMO and LUMO levels and we have neglected the possibility that the molecule can become charged. Nevertheless, our calculations demonstrate that when the Fermi energy is located far from the HOMO or LUMO resonance peaks, a threshold voltage with a value close to the one measured by Marquardt *et al.*[19] arises naturally within a phase-coherent tunneling picture of transport, of the kind discussed in Ref. 10.

The transition from noble-metal-based electrodes to carbon-based electrodes represents a paradigm shift for molecular electronics. For the future, it will be fruitful to examine a range of alternative planar anchor groups, including pyrene and pyrene derivatives, which are known to bind strongly to graphene and CNTs,[26] larger polycyclic aromatics, and molecules terminated by multiple anchor groups.

ACKNOWLEDGMENTS

We gratefully acknowledge discussions with Iain Grace and funding from the Marie-Curie ITNs FUNMOLS and NANOCTM. Funding is also provided by EPSRC and METRC.

*c.lambert@lancaster.ac.uk

[1] J. M. Tour, Acc. Chem. Res. **33**, 791 (2000); R. L. Carroll and C. B. Gorman, Ang. Chem. Int. Ed. **41**, 4378 (2002); G. Maruccio, R. Cingolani, and R. Rinaldi, J. Mater. Chem. **14**, 542 (2004); A. Troisi and M. A. Ratner, Small **2**, 172 (2006); D. K. James and J. M. Tour, Aldrichim. Acta **39**, 47 (2006); N. Weibel, S. Grunder, and M. Mayor, Org. Biomol. Chem. **5**, 2343 (2007); F. Chen, J. Hihath *et al.*, Annu. Rev. Phys. Chem. **58**, 535 (2007); H. B. Akkerman and B. Boer, J. Phys.: Condens. Matter **20**, 013001 (2008).

[2] R. L. McCreery, U. Viswanathan *et al.*, Faraday Discuss. **131**, 33 (2006); S. M. Lindsay and M. A. Ratner, Adv. Mater. **19**, 23 (2007); Y. Hu, Y. Zhu, H. Gao, and H. Guo, Phys. Rev. Lett. **95**, 156803 (2005); C. Li, I. Pobelov *et al.*, J. Am. Chem. Soc. **130**, 318 (2007).

[3] W. Haiss, H. v. Zalinge *et al.*, Faraday Discuss. **131**, 253 (2006); D. R. Jones and A. Troisi, J. Phys. Chem. C **111**, 14567 (2007).

[4] D. P. Long, J. L. Lazorcik *et al.*, Nat. Mater. **5**, 901 (2006); H. Cao, J. Jiang *et al.*, J. Am. Chem. Soc. **130**, 6674 (2008); E. Leary, H. Höbenreich *et al.*, Phys. Rev. Lett. **102**, 086801 (2009).

[5] A. Salomon, D. Cahen *et al.*, Adv. Mater. **15**, 1881 (2003); C. Wang, A. S. Batsanov *et al.*, J. Am. Chem. Soc. **131**, 15647 (2009); T. Wandlowski, V. Kaliginedi *et al.*, *ibid.* **134**, 5262 (2012).

[6] J. G. Kushmerick, D. B. Holt *et al.*, J. Am. Chem. Soc. **124**, 10654 (2002).

[7] X. Li, J. He *et al.*, J. Am. Chem. Soc. **128**, 2135 (2006).

[8] L. Venkataraman, J. E. Klare *et al.*, Nature (London) **442**, 904 (2006); F. Pauly, J. K. Viljas, J. C. Cuevas, and G. Schon, Phys. Rev. B **77**, 155312 (2008).

[9] W. Haiss, C. Wang *et al.*, Nat. Mater. **5**, 995 (2006); J. Phys.: Condens. Matter **20**, 374119 (2008).

[10] G. Sedghi, V. M. García-Suárez *et al.*, Nat. Nanotechnol. **6**, 517 (2011).

[11] R. E. Sparks, V. M. Garcia-Suarez, D. Zs. Manrique, and C. J. Lambert, Phys. Rev. B **83**, 075437 (2011); S. Ke, W. Yang, and H. U. Baranger, Nano Lett. **8**, 3257 (2008); R. Stadler, Phys. Rev. B **80**, 125401 (2009); C. A. Stafford, D. M. Cardamone, and S. Mazumdar, Nanotechnology **18**, 424014 (2007); T. Hansen, G. C. Solomon *et al.*, J. Chem. Phys. **131**, 194704 (2009).

[12] E. Lörtscher, C. J. Cho *et al.*, ChemPhysChem **12**, 1677 (2011); L. A. Zotti, T. Kirchner *et al.*, Small **6**, 1529 (2010).

[13] W. Hong, D. Z. Manrique *et al.*, J. Am. Chem. Soc. **134**, 2292 (2011).

[14] S. Ranganathan, I. Steidel *et al.*, Nano Lett. **1**, 491 (2001).

[15] Z. Cheng, R. Skouta *et al.*, Nat. Nanotechnol. **6**, 353 (2011).

[16] A. Mishchenko, M. Abdualla *et al*., Chem. Commun. **47**, 9807 (2011); G. J. Ashwell, L. J. Phillips *et al*., ACS Nano **4**, 7401 (2010).

[17] S. Wu, M. T. González *et al*., Nat. Nanotechnol. **3**, 569 (2008); S. Martin, I. Grace *et al*., J. Am. Chem. Soc. **132**, 9157 (2010); L. Lin, J. Leng *et al*., J. Phys. Chem. C **113**, 14474 (2009); L. Lin, X. Song *et al*., J. Phys.: Condens. Matter **22**, 325102 (2010).

[18] F. Prins, A. Barreiro *et al*., Nano Lett. **11**, 4607 (2011).

[19] C. W. Marquardt, S. Grunder *et al*., Nat. Nanotechnol. **5**, 863 (2010).

[20] A. Blaszczyk, M. Fischer *et al*., Helv. Chim. Acta **89**, 1986 (2006).

[21] J. M. Soler, E. Artacho *et al*., J. Phys.: Condens. Matter **14**, 2745 (2002).

[22] J. P. Perdew, K. Burke, and M. Ernzerhof, Phys. Rev. Lett. **77**, 3865 (1996).

[23] The relaxed coordinates of the CNT-molecule-CNT systems with lattice defects, together with the corresponding three-dimensional rotatable images, are available at www.lancs.ac.uk/staff/peterfal/Bulky.html

[24] A. R. Rocha, V. M. García-Suárez, S. Bailey, C. Lambert, J. Ferrer, and S. Sanvito, Phys. Rev. B **73**, 085414 (2006).

[25] A. Stone and D. Wales, Chem. Phys. Lett. **128**, 501 (1986); G. J. Dienes, J. Appl. Phys. **23**, 1194 (1952); C. Ewels, M. Heggie, and P. Briddon, Chem. Phys. Lett. **351**, 178 (2002); C. J. Lambert and D. L. Weaire, Metallography **14**, 307 (1981).

[26] S. Bailey, M. R. Bryce *et al*. (unpublished); S. D. Chakarova-Käck, A. Vojvodic *et al*., New J. Phys. **12**, 013017 (2010).